Macromolecular Research, Vol. 24, No. 1, pp 83-89 (2016)
DOI 10.1007/s13233-016-4007-7

www.springer.com/13233
pISSN 1598-5032 eISSN 2092-7673

Surface Engineering of Titanium with Simvastatin-Releasing Polymer Nanoparticles for Enhanced Osteogenic Differentiation

Jun Ho Jegal[1], Gi Hyun Choi[1], Hong Jae Lee[1], Ki Duk Kim[2], and Sang Cheon Lee*[,1]

[1]*Department of Maxillofacial Biomedical Engineering & Institute of Oral Biology, School of Dentistry, Kyung Hee University, Seoul 02447, Korea*

[2]*Department of Life and Nanopharmaceutical Science, College of Pharmacy, Kyung Hee University, Seoul 02447, Korea*

Received October 1, 2015; Revised November 9, 2015; Accepted November 13, 2015

Abstract: We describe a novel approach for surface engineering of titanium (Ti) with polymer nanoparticles that can sustainably release an osteogenic compound, simvastatin (SV). The SV-loaded nanoparticles (SV-GC-CA) were prepared by self-assembly of 5β-cholanic acid-conjugated glycol chitosan (GC-CA) in the presence of SV. Dynamic light scattering (DLS) and transmission electron microscopy (TEM) analyses showed that the SV-GC-CA nanoparticles had a hydrodynamic diameter of 371.4 nm with a spherical shape. The surface engineering of Ti was performed by pre-treatment of Ti surface with polydopamine (PD) coatings, followed by immobilization of the SV-GC-CA nanoparticles. The immobilization of the SV-GC-CA nanoparticles onto PD-treated Ti surfaces could be achieved by a simple dipping method in an aqueous solution. The successful immobilization of the SV-GC-CA nanoparticles onto Ti surfaces was confirmed by field-emission scanning electron microscopy (FE-SEM), and the density of immobilized nanoparticles could be controlled. SV was sustainably released for up to 20 days, and the release rate was dependent on the loading amount of SV. The Ti substrate functionalized with SV-releasing nanoparticles significantly promoted alkaline phosphatase (ALP) activity of osteoblast-like cells (MC3T3-E1). The surface engineering approach described in this work has an applicability for various medical devices to generate surfaces with improved osteogenic potentials.

Keywords: simvastatin, titanium, sustained release, osteogenic differentiation, surface immobilization.

Introduction

Titanium (Ti) has been extensively used as a material of great importance for orthopedic and dental implants because of its resistance to corrosion, excellent mechanical properties, and biocompatibility.[1-3] In particular, the Ti implants have been chemically, physically, or biochemically treated to improve their surface bioactivity for efficient interfacial adhesion between the bone tissue and implant surface.[4-6] The efficient adhesion at the interface is an important issue in that it can reduce the risk of an implant loosening and eventually prevent implant failure.[7,8]

Of various surface treatment methods, a recent trend has focused on the attachment of bioactive agents, such as an arginine-glycine-aspartic acid (RGD) peptide sequence and bone-inducing growth factors, onto Ti substrates.[9-11] Surface modification of Ti for improving osteoconductivity or osteoinductivity is an attractive strategy for satisfactory osseointegration of orthopedic or dental implants. Especially, treatments of Ti surfaces with surface releasing nanoparticles systems have attracted a growing interest due to their excellent performance for enhanced bone-forming or therapeutic activity.[12-16] Recently, we reported on the successful use of polymer nanoparticles for immobilization on Ti substrates so that the nanoparticles could sustainably release bone morphogenic protein-2 or insulin-like growth factors for osteogenic differentiation.[14-16] However, to date, the surface-immobilized nanoparticles for improving osteogenic differentiation was restrictively designed for the release of growth factors. Thus, there is a need for the nanoparticle surface releasing system that can release diverse classes of osteogenic speciecs including low molecular weight compounds or genetic molecules.

In this study, we suggested a novel approach for surface engineering of Ti through the immobilization of chitosan-based nanoparticles that can sustainably release a osteogenic compound, simvastatin (SV). SV was chosen as a model osteogenic low molecular weight compound, because it is known to efficiently inhibit osteoclast differentiation and simultaneously stimulate osteoblast differentiation by inhibition of the HMG-CoA reductase.[17,18] Figure 1 illustrates the overall process of our approach. First, SV was loaded into a self-assembled nanoparticle constructed from a 5β-cholanic acid-conjugated glycol chitosan (GC-CA). The nanoparicle consisted of the hydrophobic SV-loaded CA core and the hydrated GC shells. For nanoparti-

*Corresponding Author. E-mail: schlee@khu.ac.kr

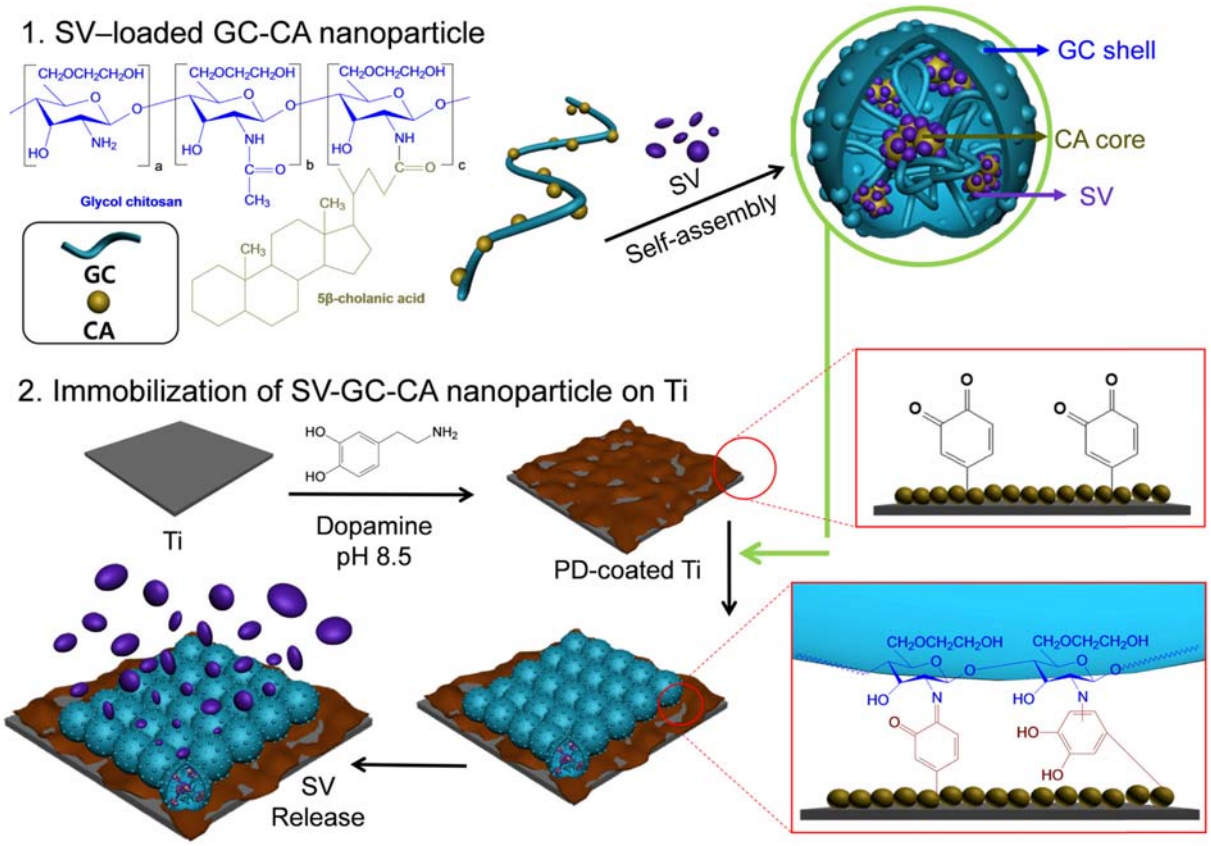

Figure 1. Schematic illustration of preparation of SV-loaded GC-CA nanoparticles, nanoparticle immobilization onto PD-coated Ti substrates, and the sustained release of SV.

cle immobilziation on Ti substrates, Ti surfaces were first treated by polydopamine (PD) coating. The surface-exposed primary amine groups of the GC shells enabled the SV-GC-CA nanoparticles to be immobilzed on the PD-treated Ti substrate by their reaction with residual quinone moieties on PD-coated Ti surfaces through Michael addition or Schiff base formation.

The formation of the SV-GC-CA nanoparticles was confirmed by dynamic light scattering (DLS) and transmission electron microscopy (TEM). X-Ray photoelectron spectroscopy (XPS) and field-emission scanning electron microscopy (FE-SEM) verified the successful immobilization of nanoparticles onto Ti surfaces. The wettability of the nanoparticle-immobilized Ti surface was analyzed by static water contact angle measurement. The release of SV from the nanoparticle-immobilized Ti surfaces was examined. The effect of SV-releasing nanoparticles on alkaline phosphatase (ALP) activity of osteoblast-like cells (MC3T3-E1) was estimated.

Experimental

Materials. GC (degree of polymerization ≥ 400), CA, *N*-hydroxysuccinimide (NHS), *N*-(3-dimethylaminopropyl)-*N*′-ethylcarbodiimide hydrochloride (EDC·HCl), dopamine hydrochloride, and hydrofluoric acid were purchased from Aldrich Co. (Milwaukee, WI). SV was obtained from Hanmi Pharm. Co. (Korea). Osteoblast-like preosteoblast cell line (MC3T3-E1) was obtained from Korean Cell Bank Line (Seoul, Korea). All other solvents and chemicals were of analytical grade and used as received.

Preparation of GC-CA. The GC-CA conjugate was synthesized by the EDC-mediated coupling reaction between the primary amine groups of GC and the carboxylic groups of CA.[19] Briefly, GC (1 g, 4.81×10^{-3} mol) and CA (122.4 mg, 0.34×10^{-3} mol) were dissolved in a distilled water/methanol co-solvent (1:1, v/v), followed by the addition of equivalent mole of NHS and EDC (0.51×10^{-3} mol). The reaction mixture was stirred at room temperature for 1 day and was then dialyzed using a membrane (molecular weight cut-off (MWCO): 3,500 g/mol) against water/methanol (1:3; 6 h → 1:1; 6 h → 3:1; 6 h, v/v) for 1 day and distilled water for 2 days, followed by freeze-drying. Yield: 78.4%.

Preparation of SV-Loaded GC-CA Nanoparticles. The SV-loaded GC-CA (SV-GC-CA) nanoparticles were prepared using a dialysis method. SV (50 mg) and GC-CA (450 mg) were dissolved in dimethylsulfoxide (DMSO), vigorously stirred for 30 min at room temperature, and dialyzed against distilled water using a membrane (MWCO (molecular weight cut off): 3,500 g/mol) for 1 day, followed by freeze-drying.

Yield: 87.2%.

Characterization of SV-GC-CA Nanoparticles. The chemical structure of GC-CA was confirmed by ^{1}H NMR (nuclear magnetic resonance) spectroscopy at 400 MHz (Varian INOVA400, USA). The loading amount of SV was calculated using a UV-Vis spectrophotometer (Shimadzu UV-1650PC, Japan). The size distribution and mean diameter of the SV-GC-CA nanoparticles were confirmed by dynamic light scattering (DLS, 90 PLUS particle size analyzer, BrookHAVEN, New York, USA). The mean hydrodynamic diameter (d) of the SV-GC-CA nanoparticles was calculated using a Stokes-Einstein equation, and the polydispersity factor (μ_2/Γ^2) was calculated using the cumulant method.[20] The zeta potential (ζ) of the nanoparticle was measured by a 90 PLUS particle size analyzer. The morphology of the SV-GC-CA nanoparticles was confirmed by TEM (CM30, Philips, CA). For sample specimens, the aqueous solution of the SV-GC-CA nanoparticles was dropped on a 200 mesh cooper grid. After 1 min, surface water was absorbed by a filter paper. The sample was stained with a 1% uranyl acetate solution. The TEM image was measured at a voltage of 200 kV.

Pretreatment of Ti Substrates with Polydopamine (PD) Coating. Ti substrates of a circle type were etched with 0.1% hydrofluoric acid after 10 min, rinsed with acetone, isopropyl alcohol, and water, and then vacuum-dried. Following a literature procedure, the etched Ti substrates were treated with a thin PD film by immersion of the Ti substrates in an alkaline dopamine·HCl solution (0.5 mg/mL of dopamine·HCl dissolved in 10 mM Tris buffer, pH 8.5) for 30 min.[21] Then, Ti substrates were rinsed with distilled water twice and then dried in vacuo.

Immobilization of SV-GC-CA Nanoparticles on Ti Substrates. The SV-GC-CA nanoparticles were immobilized onto PD-treated Ti substrates. The aqueous solutions of SV-GC-CA nanoparticle of various concentrations (1~10 g/L) were dropped on the PD-treated Ti substrates and incubated for 2 h at room temperature. After the immobilization procedure, the Ti substrates were rinsed with distilled water three times and then dried in vacuo.

Surface Characterization of SV-GC-CA-Immobilized Ti Substrates. The surface morphology of the immobilized SV-GC-CA nanoparticles onto Ti substrates was analyzed using a field-emission scanning electron microscope (FE-SEM, XL-30, FEI, Netherlands), after sputter-coating with platinum. Surface elemental compositions of the bare Ti substrate and SV-GC-CA nanoparticle-immobilized Ti substrates were observed by XPS (ESCALAB MK II, V.G. Scientific Co., UK). Each sample was examined at a pass energy of 80 eV with the anode operated at 300 W, and the percentage of the surface element was calculated by normalizing the area of each element peak with the area of total peak. Surface wettability of SV-GC-CA nanoparticle-immobilized Ti substrates was confirmed by contact angle measurements of a water droplet using a contact angle meter (Surface Electro Optics, PHOENIX 150). The mean value of water contact angles measured at five different points on the Ti surface was adopted.

Release of SV from Nanoparticle-Immobilized Ti Surface. *In vitro* release profiles of SV from the surface of SV-GC-CA nanoparticle-immobilized Ti substrates were estimated in phosphate-buffered saline (PBS) solution (pH 7.4). The SV release experimet was performed using a Ti substrates prepared using the nanoparticle concentrations of the 5 g/L and 10 g/L. The SV-GC-CA-immobilized Ti substrates were immersed in the PBS solution (3 mL) and shaken at a speed of 90 rpm at 37 °C. The release medium was completely renewed at predetermined time intervals, and all samples were stored at 4 °C until analysis. The accumulated amount of released SV was calculated by using a UV-Vis spectrophotometer.

MC3T3-E1 Cell Attachment. For attachment of osteoblast-like MC3T3-E1 cells, four groups of Ti substrates were prepared as follows: i) bare Ti, ii) dopamine-coated Ti (PD-Ti), iii) SV-GC-CA nanoparticle-immobilized Ti 1 (SV-GC-CA-Ti 1), and iv) SV-GC-CA nanoparticle-immobilized Ti 4 (SV-GC-CA-Ti 4). MC3T3-E1 cells were cultured in Dulbecco's modified Eagle medium (Gibco, Grand Island, New York, USA) with 5% CO_2 at 37 °C. Each sample was placed into 48-well plates, and MC3T3-E1 cells were seeded at a density of 10,000 cells on each substrate. The culture medium was replaced every 2 days during the whole cell culturing period. The attachment of MC3T3-E1 cells on each sample was observed after 6 h of incubation. The attachment was confirmed by counting the number of MC3T3-E1 cells with a Cell Counting Kit-8 (CCK-8) (Dojindo, Japan). The absorbance of the samples was measured by a microplate reader (Bio-Rad, Benchmark Plus) at a wavelength of 450 nm after shaking for 3 s.

Alkaline Phosphatase (ALP) Activity. The level of ALP activity was evaluated by the conversion of sodium para-nitrophenyl-2-phosphate (PNPP) to para-nitrophenol (PNP).[14] The osteogenic growth medium was supplemented with 26 μg/mL L-ascorbic acid, 10 mM β-glycerophosphate, and 10 nM dexamethasone. MC3T3-E1 cells were seeded onto various Ti substrates at a density of 20,000 cells, and the medium was replaced every 2 days. At the regular time intervals, each sample was washed with PBS and then treated with 180 mL of cell lysis buffer for 30 min. The samples were then centrifuged at 13,000 rpm for 10 min at 4 °C, and 150 μL of the sample supernatant was taken for the analysis. 50 μL of PNPP was added to each sample and incubated for 30 min at 37 °C. Next, 50 μL of 1 N NaOH solution was added to stop the reaction, and the absorbance at 405 nm was measured using a microplate reader (Bio-Rad, Benchmark Plus). The total protein concentration of the sample was also calculated by using a Bradford protein assay method. The lysed sample supernatant (2 μL) was mixed with distilled water (798 μL). The Bradford solution (5× concentrate, Bio-Rad, Hercules, CA, USA) was added into the solution, and then the absorbance was measured at 595 nm. The unit of ALP activity was presented as μM/min/μg protein.

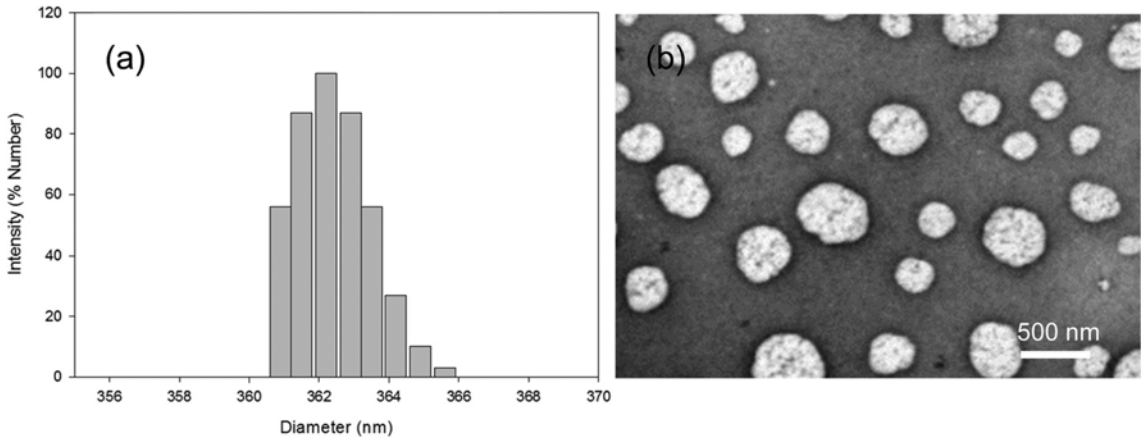

Figure 2. (a) Size distribution by DLS and (b) TEM image of SV-GC-CA nanoparticles.

Results and Discussion

Preparation of SV-GC-CA Nanoparticles. The self-assembling GC-CA conjugate was prepared following a literature procedure.[19] Using ^{1}H NMR analysis, the conjugating ratio of CA in GC was estimated to be 5.7% (Table I). In the aqueous phase, the GC-CA conjugate would self-assemble to form the nanoparticles consisting of GC shells and CA multi-cores. SV was loaded into the CA core of the GC-CA nanoparticles using a dialysis method. The mean diameter and polydispersity factor of the SV-GC-CA nanoparticles were calculated by DLS (Table II). The mean diameter (d) of the SV-GC-CA nanoparticles was 371.4 nm with a moderate size distribution (Figure 2(a)). The SV-GC-CA nanoparticle with a spherical shape was confirmed by TEM (Figure 2(b)). The zeta potential (ζ) of the SV-GC-CA nanoparticles was reasonably positive (9.2 mV) due to the cationic GC shells. The UV-Vis absorption spectra in Figure 3 shows the successful loading of SV within the CA core. The SV-GC-CA nanoparticles exhibited a higher drug loading efficiency (97.9%) with 9.8 wt% of SV loading amount (Table II).

SV-GC-CA Immobilization on PD-Pretreated Ti Substrates. The surface-exposed amine groups of the SV-GC-CA nanoparticles can play an important role in immobilization of nanoparticles onto PD-treatetd Ti substrates because of its reactivity for quinone moieties in PD-Treated Ti surfaces. For surface immobilization, aqueous solutions of the SV-GC-CA nanoparticles with various concentrations (1~10 g/L) were equilibrated with Ti substrates. Each Ti substrate was denoted as SV-GC-CA-Ti 1, SV-GC-CA-Ti 4, SV-GC-CA-Ti 5, and SV-GC-CA-Ti 10. Figure 4 shows increased nanoparticle density in SV-GC-CA-Ti 10 relative to the SV-GC-CA-Ti 5 group. This result suggests that the number of immobilized nanoparticles can be conveniently controlled by adjusting the concentration of the SV-GC-CA nanoparticle solution.

The successful immobilization of the nanoparticles onto the Ti surface was confirmed by XPS spectra (Figure 5). For PD-Ti substrates, the atomic signal of the nitrogen element,

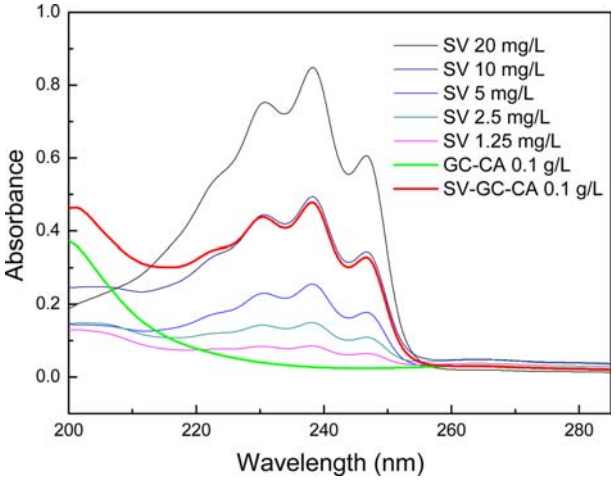

Figure 3. UV-Vis spectra of SV, the GC-CA conjugate, and the SV-GC-CA nanoparticle in anhydrous MeOH/H_2O (2:1, v/v).

Table I. Characteristics of the GC-CA Conjugate

Conjugate	Feed Ratio ([GC] : [CA])	Composition Ratio ([GC] : [CA])	Conjugation Ratio of CA[a] (%)
GC-CA	100 : 7	100 : 5	5.7

[a]Calculated by ^{1}H NMR spectra.

Table II. Characteristics of SV-GC-CA Nanoparticles

Nanoparticle	d (nm)	ζ^a (mV)	$\mu_2/\Gamma^{2\,b}$	SV Loading Content (wt%)	SV Loading Efficiency (%)
SV-GC-CA	371.4	9.2	0.19	9.8	97.9

[a]Estimated at pH 7.4. [b]Polydispersity factor by dynamic light scattering.

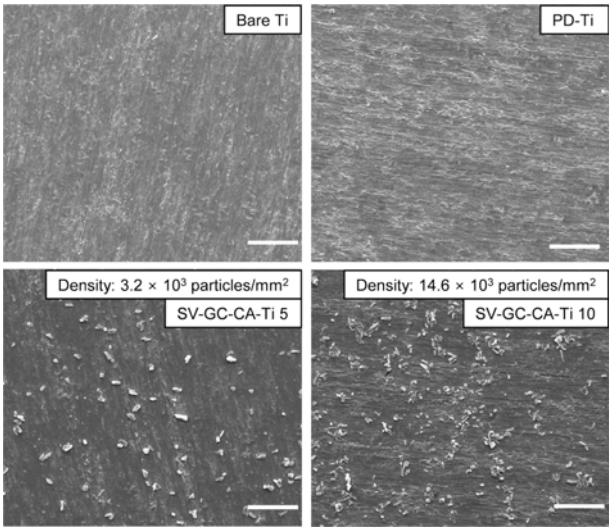

Figure 4. Surface morphology of bare Ti, PD-Ti, and SV-GC-CA-immobilized Ti substrates observed by FE-SEM. Scale bars represent 50 μm.

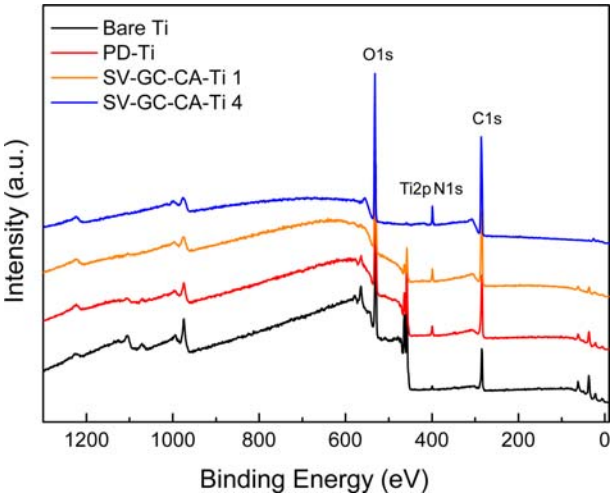

Figure 5. XPS survey spectra of bare Ti, PD-Ti, and SV-GC-CA-immobilized Ti substrates.

Table III. Surface Analysis Results of Bare Ti and SV-GC-CA Nanoparticle-Immobilized Ti Substrates

Sample	Surface Atomic Composition (%)			
	[C]	[N]	[O]	[Ti]
Bare Ti	32.8	1.4	47.7	18.0
PD-Ti	51.4	4.0	35.1	9.3
SV-GC-CA-Ti 1	60.9	4.8	30.6	3.5
SV-GC-CA-Ti 4	65.3	5.4	28.8	0.3

which was seldom found in the spectrum of bare Ti substrates, was found to be 4.0% due to the nitrogen of PD coatings. In the case of to SV-GC-CA-immobilzied Ti subtrates, the increased ratio of nitrogen was found (4.8%), and it was increased to 5.4% with increasing the nanoparticle concentration (Table III). The increased number of immobilized nanoparticles on the surface of the Ti substrates may result in an increased number of amine groups on the GC surface, which is the source of the nitrogen element. In addition, as the nanoparticle concentration used for surface immobilization increased from 1 g/L to 4 g/L, the surface atomic ratio of the Ti element decreased from 3.5% to 0.3% (Table III). This indicates that the exposed area of Ti decreased by increasing the nanoparticle density.

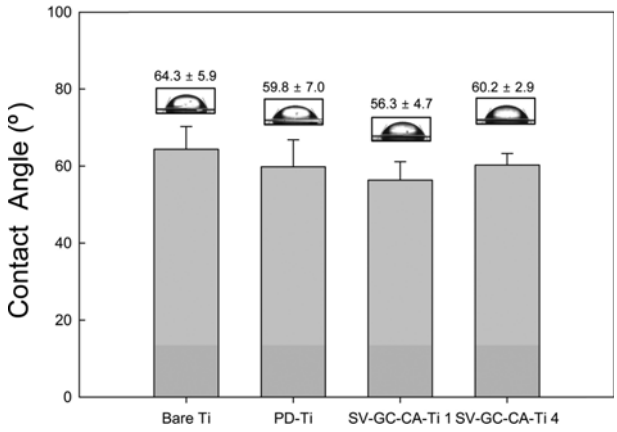

Figure 6. Static contact angles of bare Ti, PD-Ti, and SV-GC-CA-immobilized Ti substrates.

The static contact angles were estimated for nanoparticle-immobilized Ti substrates (Figure 6). The contact angle of the bare Ti was 64.3°. The contact angle was similar for SV-GC-CA-Ti 1 (56.3°) and SV-GC-CA-Ti 2 (60.2°), despite the increasing surface density of the SV-GC-CA nanoparticles.

Release of SV from SV-GC-CA Nanoparticles Immobilized on Ti Substrates. To obtain release profiles of SV, the Ti substrates were prepared using two different concentrations of SV-loaded nanoparticles, 5 g/L and 10 g/L. SV was released

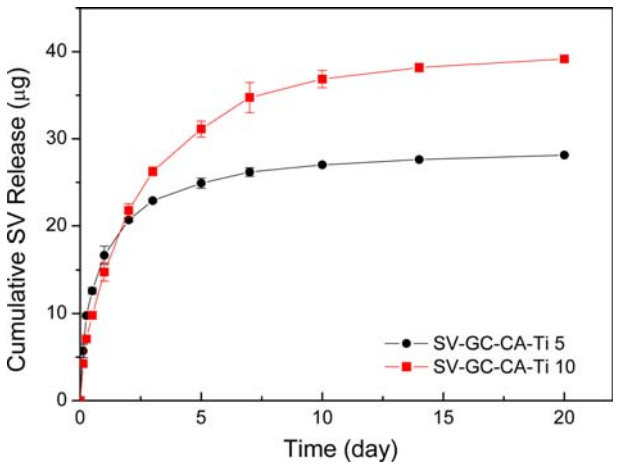

Figure 7. Cumulative *in vitro* release profiles of SV from SV-GC-CA-immobilized Ti substrates.

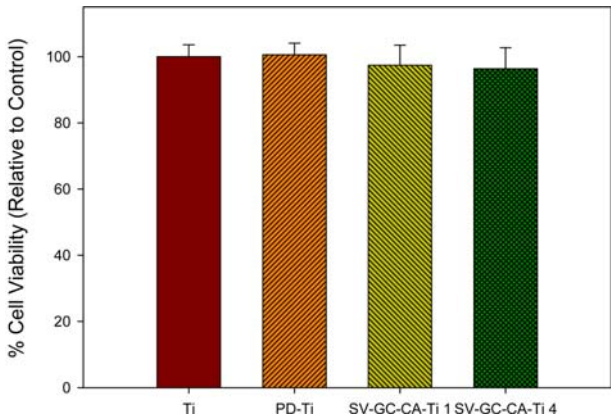

Figure 8. Attachment of MC3T3-E1 cells on surfaces of various Ti substrates.

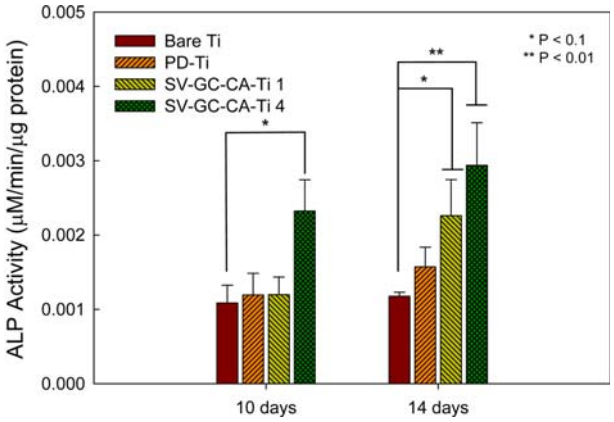

Figure 9. ALP activities of bare Ti, PD-Ti, and SV-GC-CA-immobilized Ti substrates.

in a greater amount from SV-GC-CA-Ti 10, as compared to the release amount from SV-GC-CA-Ti 5. These kinetics support the dose-dependent diffusion-based release of nanoparticles. The amount of the cumulative release of SV at 20 days was 28.1 μg from SV-GC-CA-Ti 5 and 39.2 μg from SV-GC-CA-Ti 10. The release of SV from SV-GC-CA nanoparticle-immobilized Ti substrates lasted for up to 20 days (Figure 7). The sustained release SV may efficiently promote osteogenic differentiation of MC3T3-E1 cells.

Attachment of MC3T3-E1 Cells on SV-GC-CA Nanoparticle-Immobilized Ti Substrates. The attachment of stem cells or osteoblasts on biomaterials surface is critical for cellular functions that can enhance osteogenic differentiation. To date, MC3T3-E1 cells have been used in various applications, including restoration of bone tissue function and regeneration of damaged tissues.[22-24] The attachment of MC3T3-E1 cells needs to be confirmed in order to differentiate MC3T3-E1 cells into cells that can be used for bone regeneration. The attachment on various Ti substrates was estimated by calculating the number of attached MC3T3-E1 cells after 6 h of culturing. Figure 8 shows the number of MC3T3-E1 cells adhered to the nanoparticle-immobilized Ti surfaces. The number of MC3T3-E1 cells adhered to bare Ti and PD-Ti surfaces was found to be similar. On the basis of this result, the immobilization of the SV-GC-CA nanoparticles onto Ti substrates did not provide the harmful environment for attachment of MC3T3-E1 cells.

Alkaline Phosphatase (ALP) Activities. ALP, one of the most important markers of osteogenic differentiation, is expressed in the early stage of osteoblastic cell lines.[25,26] We evaluated the ALP activity on SV-releasing nanoparticle-immobilized Ti substrates. ALP activities of various Ti substrates were estimated at pre-determined specific time points during 2 weeks. In order to examine the effect of SV on osteoblastic differentiation, ALP levels of MC3T3-E1 cells cultured on bare Ti, PD-Ti, SV-GC-CA-Ti 1, and SV-GC-CA-Ti 4 substrates were measured at 10 and 14 days (Figure 9). For all of the specimens, the ALP level increased up to 14 days. The cells cultured on SV-GC-CA-Ti 1, and SV-GC-CA-Ti 4 substrates showed significantly higher ALP activity than that of bare Ti. This result suggests that the sustained release of SV from the Ti substrates efficiently promote the osteogenic differentiation.

Conclusions

We developed a novel surface treatment approach for Ti substrates by immobilizing SV-releasing polymer nanoparticles on Ti surfaces. The SV-GC-CA nanoparticles could be chemically immobilized on the dopamine-polymerized Ti substrates. The SV-GC-CA nanoparticles were immobilized on Ti surfaces through a simple dipping process. The density of the immobilized nanoparticles was readily controlled by adjusting the concentration of the nanoparticle solution. SV was sustainably released in a controlled manner. The SV-releasing Ti substrates promoted the osteogenic differentiation. The approach described in this work may find many applications as surface controlled releasing systems for bioactive orthopedic and dental implants.

Acknowledgment. This work was supported by the National Research Foundation of Korea (NRF) grant funded by the Korea government (MSIP) (No. 2012R1A5A2051388) and was supported by a grant of the Korea Health Technology R&D project (HI14C0175) through the KHIDI funded by the Ministry of Health & Welfare, Republic of Korea.

References

(1) M. Geetha, A. Singh, R. Asokamani, and A. Gogia, *Prog. Mater. Sci.,* **54**, 397 (2009).
(2) D. A. Puleo and A. Nanci, *Biomaterials*, **20**, 2311 (1999).
(3) X. Hu, K. G. Neoh, J. Zhang, E. T. Kang, and W. Wang, *Biomaterials*, **33**, 8082 (2012).
(4) L.-H. Li, Y.-M. Kong, H.-W. Kim, Y.-W. Kim, H.-E. Kim, S.-J. Heo, and J.-Y. Koak, *Biomaterials,* **25**, 2867 (2004).
(5) Y.-T. Sul, C. B. Johansson, S. Petronis, A. Krozer, Y. Jeong,

A. Wennerberg, and T. Albrektsson, *Biomaterials,* **23**, 491 (2002).
(6) L. Le Guéhennec, A. Soueidan, P. Layrolle, and Y. Amouriq, *Dent. Mater.,* **23**, 844 (2007).
(7) H. J. Lee, J. Lee, J. T. Lee, J. S. Hong, B. S. Lim, H. J. Park, Y. K. Kim, and T. I. Kim, *J. Periodontal Implant Sci*., **45**, 120 (2015).
(8) R. C. Zheng, Y. K. Park, J. J. Cho, S. K. Kim, S. J. Heo, J. Y. Koak, and J. H. Lee, *J. Dent. Res*., **93**, 1005 (2014).
(9) M. N. Nguyen, T. Lebarbe, O. F. Zouani, L. Pichavant, M. C. Durrieu, and V. Héroguez, *Biomacromolecules*, **13**, 896 (2012).
(10) Z. Shi, K.G. Neoh, E. T. Kang, C. Poh, and W. Wang, *Tissue Eng. Part A*, **15**, 417 (2009).
(11) T. Y. Lim, W. Wang, Z. Shi, C. K. Poh, and K. G. Neoh, *J. Mater. Sci.*, *Mater. Med*., **20** 1 (2009).
(12) C. T. Lo, P. R. Van Tassel, and W. M. Saltzman, *Biomaterials*, **30**, 4889 (2009).
(13) C. T. Lo, P. R. Van Tassel, and W. M. Saltzman, *Biomaterials,* **31**, 3631 (2010).
(14) H. J. Lee, A. N. Koo, S. W. Lee, M. H. Lee, and S. C. Lee, *J. Control. Release*, **170**, 198 (2013).
(15) G. H. Choi, H. J. Lee, and S. C. Lee, *Macromol. Biosci*., **14**, 496 (2014).
(16) S. W. Lee, H. J. Lee, J. W. Lee, K.-H. Kim, J.-H. Kang, M. H. Lee, and S. C. Lee, *Colloids Surf. B: Biointerfaces*, **135**, 565 (2015).
(17) G. Mundy, R. Garrett, S. Harris, J. Chan, D. Chen, G. Rossini, B. Boyce, M. Zhao, and G. Gutierrez, *Science,* **286**, 1946 (1999).
(18) Y. Lee, M. J. Schmid, D. B. Marx, M. W. Beatty, D. M. Cullen, M. E. Collins, and R. A. Reinhardt, *Biomaterials,* **29**, 1940 (2008).
(19) K. H. Min, K. Park, Y.-S. Kim, S. M. Bae, S. Lee, H. G. Jo, R.-W. Park, I.-S. Kim, S. Y. Jeong, and K. Kim, *J. Control. Release,* **127**, 208 (2008).
(20) S. J. Lee, K. H. Min, H. J. Lee, A. N. Koo, H. P. Rim, B. J. Jeon, S. Y. Jeong, J. S. Heo, and S. C. Lee, *Biomacromolecules*, **12**, 1224 (2011).
(21) H. Lee, S. M. Dellatore, W. M. Miller, and P. B. Messersmith, *Science*, **318**, 426 (2007).
(22) J. P. St-Pierre, M. Gauthier, L. P. Lefebvre, and M. Tabrizian, *Biomaterials*, **26**, 7319 (2005).
(23) P. Qiao, J. Wang, Q. Xie, F. Li, L. Dong, and T. Xu, *Mater. Sci. Eng. C: Mater. Biol. Appl.,* **33**, 4633 (2013).
(24) K. S. Kang, S.-J. Lee, H. Lee, W. Moon, and D.-W. Cho, *Exp. Mol. Med.*, **43**, 367 (2011).
(25) G. S. Stein, J. B. Lian, and T. A. Owen, *FASEB J.*, **4**, 3111 (1990).
(26) R. Marom, I. Shur, R. Solomon, and D. Benayahu, *J. Cell. Physiol.,* **202**, 41 (2005).